

# Negative strain rate sensitivity in bulk metallic glass and its similarities with the dynamic strain aging effect during deformation

Florian H. Dalla Torre,<sup>a)</sup> Alban Dubach, Marco E. Siegrist, and Jörg F. Löffler  
Laboratory of Metal Physics and Technology, Department of Materials, ETH Zurich,  
Wolfgang-Pauli-Strasse 10, 8093 Zurich, Switzerland

(Received 15 March 2006; accepted 17 June 2006; published online 1 September 2006)

Detailed investigations were carried out on the deformation behavior of Zr-based monolithic bulk metallic glass and bulk metallic glass matrix composites. The latter, due to splitting and multiplication of shear bands, exhibits larger compressive strains than the former, without significant loss of strength. Serrated flow in conjunction with a negative strain rate sensitivity was observed in both materials. This observation, together with an increase in stress drops with increasing strain and their decrease with increasing strain rate, indicates phenomenologically close similarities with the dynamic strain aging deformation mechanism known for crystalline solids. The micromechanical mechanism of a shear event is discussed in light of these results. © 2006 American Institute of Physics. [DOI: 10.1063/1.2234309]

Deformation in metallic glasses is characterized either by homogeneous or inhomogeneous flow. Above a critical temperature (typically the glass transition temperature  $T_g$ ) homogeneous flow prevails, and deformation is either Newtonian (viscous), where the strain rate sensitivity is a unity and stresses and strain rates are low, or non-Newtonian, occurring at higher strain rates and higher corresponding stresses.<sup>1–3</sup> At lower temperatures, deformation is inhomogeneous and localized to a few shear bands. In compression tests, for example, this deformation behavior manifests itself in a serrated flow curve, where stress drops ( $\Delta\sigma$ ) correspond to single shear events.<sup>4</sup> Similarly, individual shear events have recently been correlated with the “pop-ins” observed during nanoindentation testing.<sup>5,6</sup> These discrete displacement bursts have been found to decrease in magnitude and finally disappear with increasing indentation or strain rate.<sup>7,8</sup> The authors conclude that at lower strain rates single shear bands are fast enough to accommodate the applied strain, while at higher rates multiple shear bands operate simultaneously, so that single events are no longer detectable but reflect an integrated image of the occurring flow events.

Another important observation made from mechanical tests performed on metallic glasses at different strain rates is a lowering of fracture stress upon increases in the applied strain rate.<sup>2,9,10</sup> However, due to the limited amount of plastic strain in metallic glasses, data on strain rate change tests within one specimen [providing more accurate strain rate sensitivity (SRS) values] are scarce. This work aims to remedy this situation by cycling the strain rate several times before failure and thereby provide further evidence for the origin of the stress response upon a strain rate change. In this context, close similarities in the deformation behavior of bulk metallic glasses (BMGs) with that of crystalline alloys [which also deform inhomogeneously and where deformation is described by the dynamic strain aging (DSA) mechanism] were observed.

A master alloy of composition  $\text{Zr}_{52.5}\text{Ti}_5\text{Cu}_{17.9}\text{Ni}_{14.6}\text{Al}_{10}$  (Vit105) was produced by arc-melting and subsequently cast

into rods of 3 mm in diameter.<sup>11</sup> A second batch of specimens was produced by adding 6 vol % of graphite particles to the master alloy. A more detailed description of the processing route and the resulting microstructure is provided elsewhere.<sup>12</sup> The particles have a size of 25–45  $\mu\text{m}$  and are homogeneously distributed in the amorphous matrix. X-ray diffraction and differential scanning calorimetry studies confirm the amorphous state of the two batches.

Compression test specimens of 5 mm in length were cut from these rods and the compression planes were polished to assure parallelism. Cycled strain rate compression tests were performed at room temperature on a screw-driven machine using a data acquisition rate of 20–200 Hz. A clip gauge mounted just above and below the specimen on the pistons enabled accurate displacement measurements. Figure 1 shows a stress-strain curve from a Vit105 specimen, where the strain rate was cycled between  $3.3 \times 10^{-4}$  and  $3.7 \times 10^{-3} \text{ s}^{-1}$  starting with the higher strain rate and achieving 2.5 cycles. The flow stresses reach slightly higher values at the lower strain rate, indicating a small but negative strain rate sensitivity.

An increase in stress drops with increasing strain is seen from a test at a constant strain rate [Fig. 2(a)]. A steady occurrence of smaller stress drops along with increasing

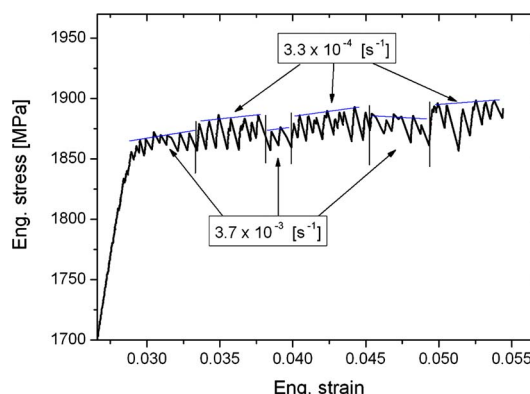


FIG. 1. (Color online) Stress-strain curves of monolithic  $\text{Zr}_{52.5}\text{Ti}_5\text{Cu}_{17.9}\text{Ni}_{14.6}\text{Al}_{10}$  (Vit105) tested at oscillating strain rates of  $3.3 \times 10^{-4}$  and  $3.7 \times 10^{-3} \text{ s}^{-1}$ .

<sup>a)</sup> Author to whom correspondence should be addressed; electronic mail: florian.dallatorre@mat.ethz.ch

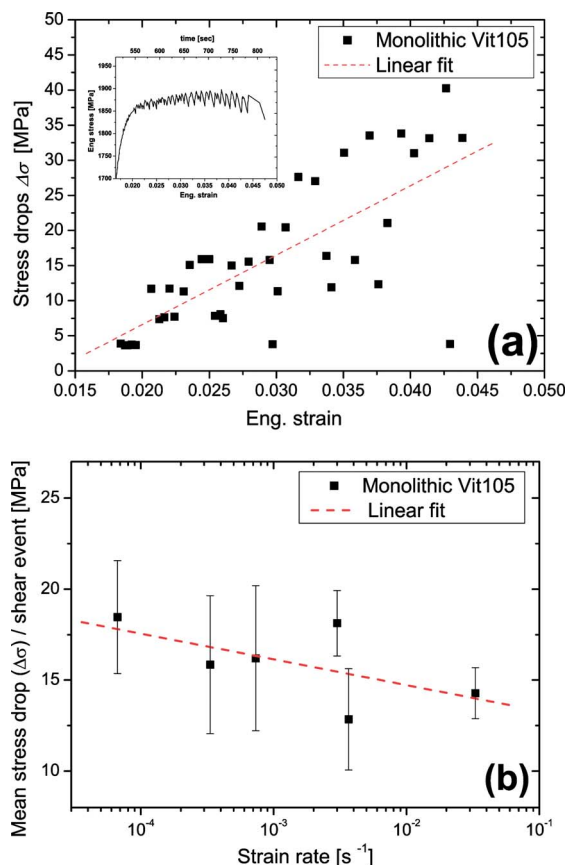


FIG. 2. (Color online) (a) Stress drops as a function of strain tested on a single Vit105 specimen at a strain rate of  $1.0 \times 10^{-3} \text{ s}^{-1}$  (the inset shows the corresponding stress-strain curve with the time scale for the duration of the test); (b) mean stress drop per shear event vs strain rate for a series of Vit105 samples.

strain is commonly observed up to intermediate strain levels. Test results on numerous monolithic samples show a decrease in the amplitude of the stress drops per average shear event with increasing strain rate [Fig. 2(b)]. The same trend was observed previously in nanoindentation and compression tests on BMGs.<sup>7,10</sup> The time needed for a stress drop occurrence increases with increasing stress drops from 10–40 ms at low stress drops (5–10 MPa) to ~100 ms at the highest stress drops (~40 MPa).

One of the main difficulties in describing deformation processes in metallic glasses is the limited number of shear events yielding low plastic strain before failure. However, in metallic glass composites, foreign particles contribute to the deformation mechanism passively by reducing stress concentrations and splitting up new shear bands, resulting in greater strains.<sup>12,13</sup> These composites are therefore ideal model materials for better understanding the microscopic deformation process occurring in metallic glasses. Figure 3 shows a stress-strain curve of a graphite-reinforced BMG. Compared to the monolithic Vit105 samples, significantly smaller stress drops but a greater number of shear events per time interval ( $t_w$ ) occur for the same strain rate and strain. This can be attributed to graphite particles, which act as potential sites where shear bands can split and multiply, so that the accumulated strain accommodated by each shear band is smaller. Analogous to the monolithic Vit105 samples, an increase in stress drops with increasing strain is observed from values of ~0.5 MPa to values as large as 50 MPa. Correspondingly

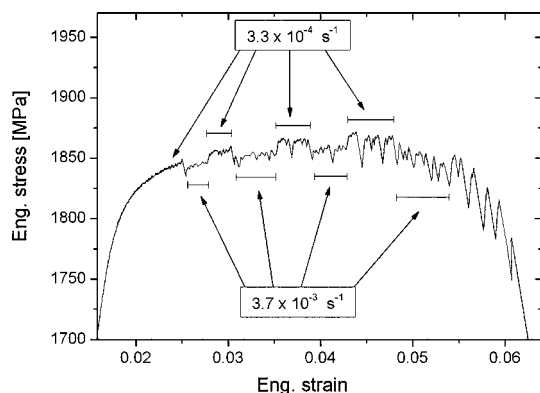


FIG. 3. Stress-strain curve of a Vit105 composite (reinforced with 6 vol % graphite particles) tested at alternating strain rates of  $3.3 \times 10^{-4}$  and  $3.7 \times 10^{-3} \text{ s}^{-1}$ .

the strain in a single shear band increases with deformation from  $\sim 10^{-5}$  to  $\sim 10^{-3}$  strain. This accompanies a decrease in the frequency of shear events ( $1/t_w$ ) with increasing strain.

A second evident point in the stress-strain curve shown in Fig. 3 is the drop in flow stress upon increasing strain rate. This behavior is presented in more detail in Fig. 4, where for monolithic Vit105 and Vit105 samples containing 6 vol % graphite the SRS defined by  $m = (\partial \ln \sigma / \partial \ln \dot{\epsilon})_{\epsilon}$  is shown as a function of the strain rate. We observed that both batches indicate low, but negative strain rate sensitivity. Due to the smaller changes in the stress upon changes in strain rate and due to significantly higher stress drops (at constant deformation speed) occurring in monolithic Vit105, the estimate of the SRS as a function of strain rate is obscured. However, a decrease in SRS with increasing strain rate is observed in the Vit105 samples containing 6 vol % graphite.

A similar negative dependence of the stress upon a change in the strain rate is seen in the dynamic strain aging phenomena in crystalline metals, where solute atoms interact with moving dislocations and macroscopically lead to Portevin–Le Châtelier deformation bands. In the now generally accepted DSA model of Mulford and Kocks,<sup>14</sup> solute atoms diffuse from forest dislocations along the core of mobile dislocations, such that the latter are pinned by the solutes before they are released at higher stress, causing a burst in strain and a stress drop. This leads to a negative SRS, which is a necessary condition for inhomogeneous serrated flow deformation in various Ni and Al alloys.<sup>14–16</sup> In these alloys

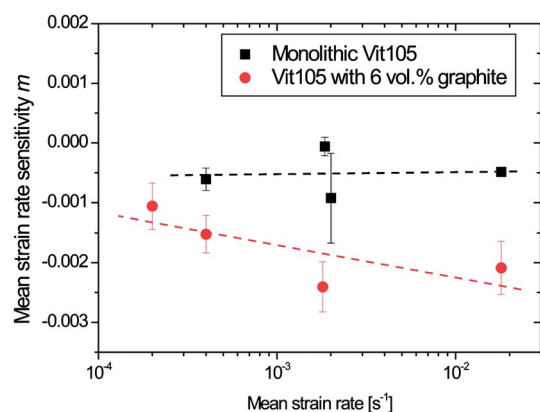


FIG. 4. (Color online) Mean strain rate vs strain rate sensitivity of monolithic Vit105 and Vit105 composites (reinforced with 6 vol % graphite particles).

different types of serrated flow can be distinguished.

In the composite samples we observed two families of serrations, a few larger ones and many smaller ones, which in appearance are comparable to the type A and B serrations in Al–5Mg.<sup>16</sup> A further similarity of our observations to the DSA mechanism is the observed increase in serration amplitude with strain [Fig. 2(a)] and a decrease in stress drops  $\Delta\sigma$  with increasing strain rate [Fig. 2(b)].<sup>14</sup> One reason for a larger  $\Delta\sigma$  and therefore higher effectiveness of the DSA mechanism with increasing strain is in Ref. 15 associated with the increased vacancy population and solute diffusivity produced during deformation such that dislocations are pinned more effectively. The increasing waiting time  $t_w$  between two serrations with increasing strain, which we also observed in this study [see inset to Fig. 2(a)], has been correlated in Ref. 14 with the enhanced ability of solute-clustering around forest dislocations. The decrease in  $\Delta\sigma$  with increasing strain rate in DSA-deforming materials has also been explained by considering the stress relaxation in the vicinity of a band.<sup>15</sup> The necessary relaxation time or the time required to build up stresses at the shear-band front and release them afterwards is lowered at higher strain rates, and thus results in a lower energy of the shear event and therefore lower  $\Delta\sigma$ .<sup>15</sup>

Despite the fundamental difference between deformation in crystalline and amorphous metals (the latter lack dislocation-mediated plasticity), the above comparison of deformation in BMGs and the DSC mechanism suggests that the phenomenological similarities found for both classes of metals may stem from a similar micromechanical origin. This may be regarded as a diffusive type of atomic rearrangement which if sufficient time is provided causes a strengthening of the shear bands leading to a higher macroscopic stress value. In metallic glasses inhomogeneous deformation is localized to “flow defects” or “shear transformation zones” comprising small groups of atoms, which cause a local rearrangement of the surrounding atomic structure and triggers the formation of macroscopic planar shear bands.<sup>17–20</sup> Studies on the structural change induced during inhomogeneous deformation have shown that higher concentrations of vacancy-like free volume defects are generated in shear bands as compared to nondeformed material (Ref. 21 and references therein), in accordance with Spaepen’s model.<sup>17</sup> If the time for a structural rearrangement or relaxation (diffusion) of free volume within shear bands and adjacent areas is sufficient after a shear displacement, the yield strength is higher, but it decreases if less time, i.e., a higher strain rate, is applied. This causes a negative SSR.

Assuming further that the larger free volume concentration within shear bands increases with increasing strain due to the occurrence of former shear events lends credence to the observed increase in the stress drops with strain and fits the common scenario of local “softening” in shear bands. The higher the free volume concentration becomes, nourished by repeated activation of the same shear band or zone, the larger the stress drops grow during deformation. This accords with our observation of few shear bands of large shear displacements surrounded by many shear bands with very small displacements. These smaller shear displacements are believed to correspond to the smaller serrations in the stress-strain curve.

This concept of inhomogeneous deformation in metallic glass differs from the model, which explains the stress drops

and shear bursts from a rheological point of view. In this model, suddenly released built-up stresses cause adiabatic heat bursts in such a way that the viscosity of the material is lowered to a level promoting further shearing along these zones (e.g., Ref. 21 and references therein). During shearing the shear rate would then first increase due to a drop in viscosity but would cease as soon as the energy supplied by the adiabatic heat is exhausted, and the free volume generated during deformation would be frozen in. It is known that fracture surfaces do exhibit viscous flow features arising from local adiabatic heat bursts, but so far it is still under debate whether such high temperatures can be expected in shear bands before failure.<sup>22–24</sup>

In conclusion, we have shown that despite their fundamental differences in structure several phenomenological similarities exist between inhomogeneous deformation in BMG’s and crystalline solids (which deform via the DSA mechanism and exhibit Portevin–Le Châtelier bands). These similarities are seen in the occurrence of serrated flow, a negative strain rate sensitivity, a decrease and increase in the stress drop amplitude ( $\Delta\sigma$ ) with increasing strain rate and strain, respectively, and an increase in the waiting time with increasing strain during compressive deformation. Since diffusion of free volume is a strong function of temperature, it is now important to further explore the role of temperature in the deformation mechanism of metallic glasses in order to more thoroughly understand the role of waiting time, stress drop magnitude, and strain rate sensitivity.

This work was supported by the Swiss National Science Foundation Under Grant No. 200021-105647 to one of the authors (F.H.D.T) and Grant No. 200021-108071 to another author (A.D.). Thanks are due to L. C. Phillips for his help with the compression tests.

<sup>1</sup>H. S. Chen and M. Goldstein, J. Appl. Phys. **43**, 1642 (1972).

<sup>2</sup>Y. Kawamura, T. Shibata, A. Inoue, and T. Masumoto, Scr. Mater. **37**, 431 (1997).

<sup>3</sup>J. Lu, G. Ravichandran, and W. L. Johnson, Acta Mater. **51**, 3429 (2003).

<sup>4</sup>H. Kimura and T. Masumoto, Acta Metall. **31**, 231 (1983).

<sup>5</sup>W. J. Wright, R. Saha, and W. D. Nix, Mater. Trans., JIM **42**, 642 (2001).

<sup>6</sup>B. Moser, J. Kübler, H. Meinhard, W. Muster, and J. Michler, Adv. Eng. Mater. **7**, 388 (2005).

<sup>7</sup>C. A. Schuh and T. G. Nieh, Acta Mater. **51**, 87 (2003).

<sup>8</sup>W. H. Jiang and M. Atzmon, J. Mater. Res. **18**, 755 (2003).

<sup>9</sup>T. Masumoto and R. Maddin, Acta Metall. **19**, 725 (1971).

<sup>10</sup>T. Mukai, T. G. Nieh, Y. Kawamura, A. Inoue, and K. Higashi, Intermetallics **10**, 1071 (2002).

<sup>11</sup>A. A. Kündig, J. F. Löffler, W. L. Johnson, P. J. Uggowitzer, and P. Thiyagarajan, Scr. Mater. **44**, 1269 (2001).

<sup>12</sup>M. E. Siegrist and J. F. Löffler, Phys. Rev. Lett. (submitted).

<sup>13</sup>A. Inoue, W. Zhang, T. Tsurui, A. R. Yavari, and A. L. Greer, Philos. Mag. Lett. **85**, 221 (2005).

<sup>14</sup>R. A. Mulford and U. F. Kocks, Acta Metall. **27**, 1125 (1979).

<sup>15</sup>J. M. Robinson and M. P. Shaw, Int. Mater. Rev. **39**, 113 (1994).

<sup>16</sup>E. Pink and A. Grinberg, Acta Metall. **30**, 2160 (1982).

<sup>17</sup>F. Spaepen, Acta Metall. **25**, 407 (1977).

<sup>18</sup>A. S. Argon, Acta Metall. **27**, 47 (1979).

<sup>19</sup>J. Saida, A. D. H. Setyawan, H. Kato, and A. Inoue, Appl. Phys. Lett. **87**, 151907 (2005).

<sup>20</sup>C. A. Schuh and A. C. Lund, Nat. Mater. **2**, 449 (2003).

<sup>21</sup>K. M. Flores, Scr. Mater. **54**, 327 (2006).

<sup>22</sup>J. J. Lewandowski and A. L. Greer, Nat. Mater. **5**, 15 (2006).

<sup>23</sup>C. J. Gilbert, J. W. Ager III, V. Schroeder, R. O. Ritchie, J. P. Lloyd, and J. R. Graham, Appl. Phys. Lett. **74**, 3809 (1999).

<sup>24</sup>B. Yang, M. L. Morrison, P. K. Liaw, R. A. Buchanan, G. Wang, C. T. Liu, and M. Denda, Appl. Phys. Lett. **86**, 141904 (2005).